ERDC/CRREL TR-16-12

US Army Corps
of Engineers®
Engineer Research and
Development Center

ERDC
INNOVATIVE SOLUTIONS
for a safer, better world

ERDC's Center-Directed Research Program—FY2015

Evaluation of Electromagnetic Induction (EMI) Resistivity Technologies for Assessing Permafrost Geomorphologies

Benjamin E. Barrowes and Thomas A. Douglas

August 2016

Cold Regions Research
and Engineering Laboratory

The U.S. Army Engineer Research and Development Center (ERDC) solves the nation's toughest engineering and environmental challenges. ERDC develops innovative solutions in civil and military engineering, geospatial sciences, water resources, and environmental sciences for the Army, the Department of Defense, civilian agencies, and our nation's public good. Find out more at www.erdc.usace.army.mil.

To search for other technical reports published by ERDC, visit the ERDC online library at http://acwc.sdp.sirsi.net/client/default.

ERDC/CRREL TR-16-12
August 2016

Evaluation of Electromagnetic Induction (EMI) Resistivity Technologies for Assessing Permafrost Geomorphologies

Benjamin E. Barrowes

U.S. Army Engineer Research and Development Center (ERDC)
Cold Regions Research and Engineering Laboratory (CRREL)
72 Lyme Road
Hanover, NH 03755-1290

Thomas A. Douglas

U.S. Army Engineer Research and Development Center (ERDC)
Cold Regions Research and Engineering Laboratory (CRREL)
Alaska Projects Office
Building 4070, 9th Street
Fort Wainwright, AK 99703

Final Report

Prepared for The ERDC Director's Office
3909 Halls Ferry Road
Vicksburg, MS 39180-6199

Under ERDC Center-Directed Research, "Integrated Technologies for Delineating Permafrost and Ground-State Conditions"

Abstract

Effective and efficient mapping of permafrost subsurface composition at scales relevant to the design and maintenance of horizontal and vertical infrastructure has been a long-standing challenge. Of utmost utility would be the development of standoff measurement techniques that could discern at the meter to submeter spatial scale and up to 10 m into the subsurface the presence or absence of ice features. Ground-based geophysical measurement techniques, including ground penetrating radar, borehole logging, and electrical resistivity, have been used to interrogate the subsurface in permafrost terrains at the meters to kilometers scales. Airborne measurement techniques have broad applicability at the larger, kilometers to tens of kilometers scale and could support linear infrastructure development and terrain mapping. However, there is a broad need for cost-effective airborne geophysical techniques to obtain high-resolution measurements of specific areas of interest.

This report explores the potential application of airborne EMI methods for the investigation and mapping of permafrost and reviews current Engineer Research and Development Center (ERDC) EMI survey capabilities and new opportunities, including the development of a new medium-scale autonomous EMI instrument.

Contents

Illustrations

Figures

Tables

Preface

This study was conducted for the Engineer Research and Development Center's (ERDC) Center-Directed Research Program under the project titled "Integrated Technologies for Delineating Permafrost and Ground-State Conditions." The technical monitor was Dr. Mark Moran, Technical Director, ERDC Cold Regions Research and Engineering Laboratory (CRREL).

The work was performed by Benjamin Barrowes (Signature Physics Branch, Dr. Loren Wehmeyer, Acting Chief) and Thomas Douglas (Biogeochemical Sciences Branch, Dr. Justin Berman, Chief), ERDC-CRREL. At the time of publication, Dr. Loren Wehmeyer was Chief of the Research and Engineering Division. The Deputy Director of ERDC-CRREL was Dr. Lance Hansen, and the Director was Dr. Robert Davis.

COL Bryan S. Green was the Commander of ERDC, and Dr. Jeffery P. Holland was the Director.

Acronyms and Abbreviations

AEM	Airborne Electromagnetics
AC	Alternating Current
BEAR	Berkley Aerial Robots
CCR	Capacitively Coupled Resistivity
CRREL	U.S. Army Cold Regions Research Engineering Laboratory
DC	Direct Current
EC	Electrical Conductivity
EMI	Electromagnetic Induction
EPA	Environmental Protection Agency
ERDC	Engineer Research and Development Center
FDEM	Frequency Domain Electromagnetics
GCR	Galvanic Contact Resistivity
GPS	Global Positioning System
GSL	Geotechnical and Structures Laboratory
MCMC	Markov Chain Monte Carlo
NAPL	Non-Aqueous Phase Liquids
ppm	Parts per Million
R&D	Research and Development
SERDP	Strategic Environmental Research and Development Program
TAPS	Trans-Alaska Pipeline System
TDEM	Time Domain Electromagnetics
UAV	Unmanned Aerial Vehicle
USGS	U.S. Geological Survey
UXO	Unexploded Ordnance

Unit Conversion Factors

Multiply	By	To Obtain
Acres	4,046.873	square meters
miles (U.S. statute)	1,609.347	meters

1 Introduction

1.1 Background

Permafrost, a cryotic soil that remains below 0°C for two or more years, is a predominant physical feature of the Earth's Arctic and subarctic regions and is therefore a major consideration for infrastructure site placement and subsequent engineering design. Permafrost underlies 22.8 million km^2 (one quarter) of the northern hemisphere's land area (Zhang et al. 2005). Permafrost, or perennially frozen ground, is estimated to cover about 85% of the state of Alaska where both continuous and sporadic discontinuous permafrost are present (Abraham 2011). In interior Alaska, almost all major infrastructure projects must account for the presence of discontinuous permafrost underlying a complex mosaic of terrains and habitats. A road, structure, or pipeline might be constructed over both frozen and unfrozen ground, affecting the types of materials and engineering approaches that are required to sustain the infrastructure. A classic example of this is the Trans-Alaska Pipeline System (TAPS), which crosses both frozen and unfrozen materials along its 1300 km route from the Arctic Ocean south to Valdez.

Effective and efficient mapping of the subsurface composition of discontinuous permafrost at scales relevant to both horizontal and vertical infrastructure has been a long-standing challenge. Mean annual temperatures in interior Alaska, currently –1°C, have increased 3°C in the past 30 years and are projected to increase an additional 5°C over the next 80 years (Chapman and Walsh 2007). This continued warming is expected to initiate widespread permafrost degradation and to alter hydrology, soil chemistry, vegetation, and microbial communities (Racine and Walters 1994; Walker et al. 2006; Wolken et al. 2011). A better understanding of the dynamic distribution and physical properties of both continuous and discontinuous permafrost will provide knowledge of how the permafrost environment may change in the future, and this understanding will subsequently drive engineering and natural resource design and response strategies.

This report focuses on using electrical conductivity (EC) measurements to map permafrost regions via surveys of the underlying substrate using electromagnetic induction (EMI; see Section 2). Section 2.1 includes a basic

review of EMI physics, and Section 3 presents specific examples of both an airborne EMI systems and a human-portable system. A discussion of current capabilities and future opportunities relevant to the Engineering Research and Development Center (ERDC) is provided in Section 4 and is followed by a conclusion section that summarizes the Report's findings.

1.1.1 Electrical conductivity (EC) of permafrost

Several studies have reported EC values of permafrost by using either electrical or EMI methods (see Figure 1 for a summary of resistivity interrogation methods). Unconsolidated deposits (such as silty sand or fluvial gravel) that are partly or fully saturated with fresh water in their pore matrix have been generally reported to yield EC values above 2 mS/m in unfrozen states and below 2.9 mS/m in frozen states (Hoekstra et al. 1975; Hauck and Kneisel 2008; Minsley et al. 2012a). An exception to this occurs with the presence of clays, which can lead to values as high as 100 mS/m when unfrozen (Minsley et al. 2012a) and as high as 20 mS/m when frozen. The presence of saline water, which strongly increases the EC of the sediments and lowers its freezing point, can lead to EC values ranging between 50 and 125 mS/m, as observed near Barrow, AK (Yoshikawa et al. 2004), or even as high as 1000 mS/m (Overduin et al. 2012). When frozen, saline permafrost regions have led to EC values as high as 50 mS/m (e.g., Overduin et al. 2012). This provides a challenge in using EC measurements to investigate highly brackish or saline regions along the coasts. For contiguous regions where permafrost is believed to be present, changes in the conductivity that are not accountable to other factors (see Section 2.2) are likely specific to permafrost.

Figure 1. A grouping diagram of methods used to investigate the electrical conductivity of the subsurface (Allen 2007).

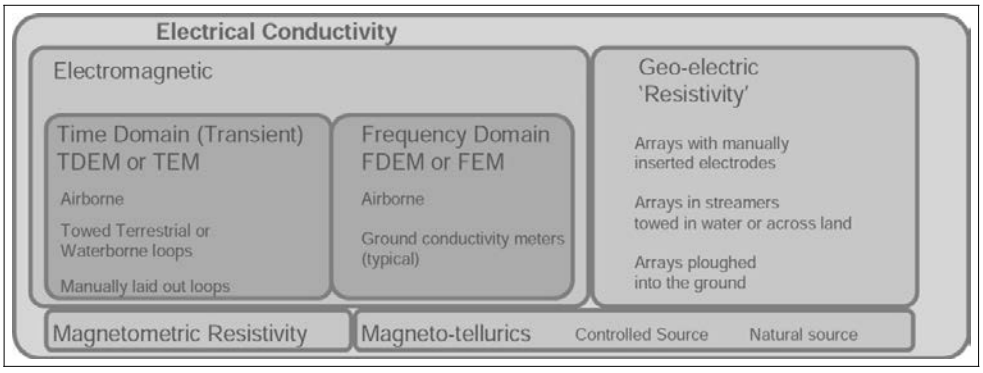

FDEM = Frequency Domain Electromagnetics

TDEM = Time Domain Electromagnetics

1.1.2 EC survey methods

Three principal near-surface geophysical methods are available for rapid, continuous measurement of the apparent EC of soil and permafrost. These methods are EMI, capacitively coupled resistivity (CCR), and galvanic contact resistivity (GCR). Section 2 will describe EMI in more detail, but below briefly describes CCR and GCR. For a review of other surface survey methods, see the U.S. Environmental Protection Agency (U.S. EPA 2014a) and Osterkamp et al. (1980).

CCR uses capacitive coupling (by using coaxial cables) to introduce electric current into the ground. A large capacitor is formed by the coaxial cable and the soil surface. The metal shield of the coaxial cable is one of the capacitor plates, and the soil surface is the other capacitor plate. The outer insulation of the coaxial cable acts as the dielectric material separating the two plates. For the transmitter, application of alternating current (AC) to the coaxial cable side of the capacitor results in an alternating current being generated in the soil on the other side of the capacitor. With regard to the receiver, the current starts in the ground and charges the capacitance of the coaxial cable, where it is measured to determine the voltage generated by the current flowing in the soil. Two transmitter coaxial cables are incorporated into the transmitter dipole, and two receiver coaxial cables are incorporated into the receiver dipole, allowing the CCR method to mimic the dipole–dipole electrode array of the more traditional GCR method. This similarity to a GCR dipole–dipole electrode array enables the CCR method to calculate apparent soil resistivity and its inverse, apparent soil EC, by using the measured electric current, measured voltage, coaxial cable dipole lengths, and the spacing distance between the two dipoles. The spacing between the two dipoles governs the soil investigation depth when the dipole lengths are kept constant. One common instrument for CCR measurements is the Geometrics Inc. OhmMapper TR1. For more information regarding CCR, see Kuras et al. (2006) and Auken et al. (2006).

GCR, or surface electrical resistivity, surveying is based on the principle that the distribution of electrical potential in the ground around a current-carrying electrode depends on the electrical resistivities and the distribution of the surrounding soil and rock material. The usual practice in the field is to apply an electrical direct current (DC) between two electrodes

implanted in the ground and then measure the difference in potential between two additional electrodes that do not carry current. Usually, the potential electrodes are in line between the current electrodes; but in principle, they can be located anywhere along or near the array. The current used is either DC, commutated direct current (i.e., a square-wave AC), or AC of low frequency (typically about 20 Hz). All analysis and interpretation are done on the basis of direct current measurements. The distribution of potential can be related theoretically to ground resistivity values and their configuration for some simple cases, notably, the case of a horizontally stratified ground and the case of homogeneous masses separated by vertical planes (for example, a vertical fault with a large throw or a vertical dike). For other kinds of resistivity distributions, interpretation is usually done by qualitative comparison of observed response with that of idealized hypothetical models or on the basis of empirical methods (U.S. EPA 2014b).

1.2 Objectives

The objective of this report is to explore the potential application of airborne EMI methods for the investigation and mapping of permafrost and to review current Engineer Research and Development Center (ERDC) EMI survey capabilities and new opportunities, including the development of a new medium-scale autonomous EMI instrument.

1.3 Approach

This report combines the authors' expertise in EMI and arctic permafrost and looks to understand the current state of the research in medium-scale EMI surveys. Specifically, the intent is to propose a new medium-scale airborne EMI survey system able to at once survey rapidly from the air but be cost effective compared to helicopter-based methods.

2 Electromagnetic Induction (EMI)

Electromagnetic induction (EMI) is a technique that can rapidly and effectively estimate the electrical conductivity of subsurface materials to a depth of 150 m without physically contacting the surface. The electrical conductivity measurements made by EMI can be used to infer the frozen or unfrozen state of earth material due to the contrast in conductivity measurements between frozen and unfrozen media. Various modalities for acquiring EMI measurements exist depending on the scope and timescale required for a given survey. These include airborne, vehicle, cart, snowmobile, boat, or handheld platforms. Airborne EMI techniques have the potential to measure terrain conditions at the tens of kilometers scale, in a single day and during all seasons.

The EMI technique involves producing a primary field at low frequencies, usually less than 100 kHz. Eddy currents are induced in conducting media by this primary field, and these eddy currents thereby produce a secondary field that can be detected by a receiver coil. These primary and secondary coils can be in a fixed geometry with respect to one another or separate and carried by different people (i.e. with a Geonics EM-34 [Geonics Limited 2014]). The following sections present greater background information on the fundamentals of EMI.

Advantages of EMI systems include the following:

- Time Domain Electromagnetics (TDEM) systems may be used in many different configurations.
- A pulsed transmitter waveform allows the receiver to measure the electromagnetic response during the transmitter off time without the presence of the primary field.
- No direct electrical contact with the ground is required, so surveys can be equally effective in frozen environments and over complex terrain where travel over the ground surface is limited.
- The same basic techniques can be used to investigate the top few meters of ground or to depths of over 1000 m.
- EMI measurement campaigns are generally fast and cost effective for the amount of data generated.

- Frequency domain systems can use multiple frequencies at once for different depth sensitivity.
- They are less sensitive to conductivity conditions at the ground surface.
- There is no problem with coupling to the ground because the EMI system is inductive.
- They can be deployed on airplane, helicopter, boat, cart, sled, vehicle, or handheld platforms.
- EMI instruments can be deployed in all seasons and soil conditions.

2.1 Basic physics of EMI

The transmitter coil induces circular eddy-current loops in the soil with the magnitude of these loops directly proportional to the electrical conductivity in the vicinity of that loop. Each secondary eddy-current loop generates a secondary electromagnetic field that is proportional to the value of the current flowing within the loop. The receiver coil of the instrument intercepts a fraction of the secondary induced electromagnetic field from each loop, and the sum of these signals is amplified and formed into an output voltage that is related to a depth-weighted soil EC. The amplitude and phase of the secondary field will differ from those of the primary field as a result of the soil's properties (e.g., clay content, water content, salinity, and frozen state; see Section 2.2); the spacing of the coils; and their orientation, frequency, and distance from the soil surface (Corwin and Lesch 2005; Corwin and Plant 2005; Ao 2001; Barrowes 2004; Ward and Hohmann 1988). Figure 2 illustrates these physical phenomena by showing the secondary fields produced from a discrete target (in this case, unexploded ordnance [UXO]). For a distributed conductivity medium such as a soil, the secondary fields are produced by the bulk medium; and conductivity profiles must be extracted from the data (see Section 2.2).

The secondary field can be converted to components in phase and 90° quadrature with respect to the transmitted field. The quadrature component, using certain simplifying assumptions, can be converted to a measure of apparent ground conductivity. The in-phase component, while generally not responsive to changes in bulk conductivity, is especially responsive to discrete, highly conductive bodies, such as metal objects. The in-phase response also can help extract the susceptibility of the background medium so that more accurate EC can be extracted from the data. The apparent conductivity measurement is the average conductivity of one

or more layers in the ground in the proximity of the instrument to a depth of investigation dependent on the coil spacing, coil orientation, operating frequencies of the instrument, and the individual conductivity of each ground layer.

Figure 2. EMI instrument conceptual operation. The primary fields (*red*) produce secondary fields (*blue*) that are detected by the receiver coil.

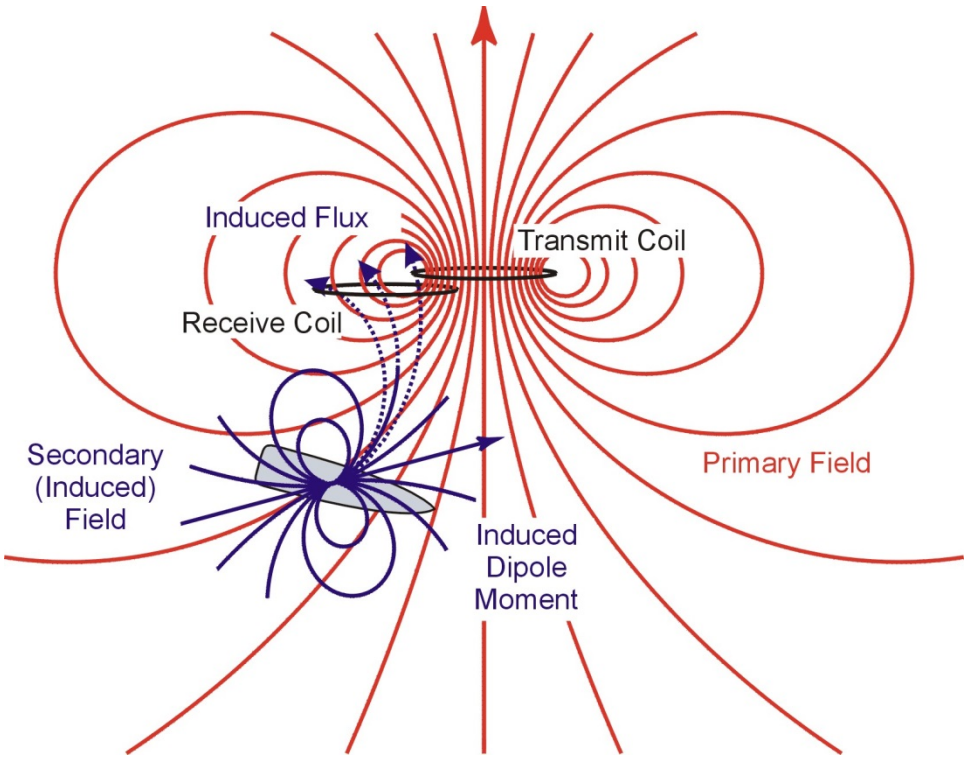

2.2 EC inversion from EMI data

FDEM data are commonly acquired from airborne and ground-based systems to provide spatially continuous information about subsurface electrical resistivity variability. To provide quantitative information about subsurface resistivity structures, the EM data must be inverted to recover the true distribution of resistivity values with depth in the subsurface.

Electrical conductivity was traditionally derived from helicopter-borne EMI data by using the pseudo-layer half-space model of Fraser (Fraser 1978). In fact, the Fugro Resolve system (Fugro Airborne Surveys 2010), summarized in Section 3.1, still uses this model for its own calculations. This model yields the apparent conductivity and the apparent sensor–

source distance directly from a transformation of the in-phase and quadrature components. The EM airborne platform altitude is not used. The pseudo-layer is merely an artifice to account for differences between the computed sensor–source distance and the measured bird altitude. Later, magnetic susceptibility was considered in the half space model, which increased the accuracy of the calculated EC (Huang and Fraser 2000). More recent models accommodate multiple permeable and conductive layers (Huang and Fraser 2003; Huang and Won 2003; Minsley et al. 2012a).

Many factors can potentially influence the apparent conductivity of the subsurface, including

- the frozen or unfrozen state of the ground,
- mineralogy (e.g., clay content),
- moisture content,
- porosity,
- the EC of subsurface water,
- stratigraphy,
- structure,
- temporal changes (e.g., soil moisture, water table, and temperature),
- adding or subtracting soluble constituents/contaminants source strength variations and directions of ground water flow, and
- the presence of non-aqueous phase liquids (NAPLs).

These factors should be accounted for when considering the inverted apparent EC of a region from a survey. Typically, assumptions about most of these variables are made during the inversion process. This results in EC values that depend strongly on the subsurface property under consideration.

The actual depth of investigation for a given frequency is an important issue regarding EC measurement with EMI methods. The skin depth, δ, occurs at the level beneath the instrument where the amplitude of the primary EM field is reduced to 1/e, or 37%, of the value generated at the transmitting coil (Reynolds 2011; Sharma 1997). The skin depth is sometimes used as an indication of the investigation depth for EMI measurement, and its value (in meters) is expressed as (Allred et al. 2006)

$$\delta = \sqrt{\frac{2}{\omega\sigma\mu_0}} \approx 504\sqrt{\frac{1}{\sigma f}}$$

where

ω = the frequency in radians/s,
σ = the conductivity in S/m,
μ_0 = the magnetic permeability of free space in Henries/m, and
f = the frequency in Hz.

The depth of exploration for a given earth medium is therefore determined by the operating frequency. As a consequence, measuring the earth response at multiple frequencies is equivalent to measuring the earth response from multiple depths. These data can be used to create a three-dimensional image of the distribution of the subsurface conductivity measurements. The inversion procedure used to extract these conductivity depth profiles relies on a full solution based on Maxwell's equations directly as opposed to one based on approximations (Dafflon et al. 2013).

Recently developed approaches estimate EC from EMI data, including a smooth one-dimensional inversion approach (Dafflon et al. 2013; Farquharson 2000; Hendrickx et al. 2002; Huang and Won 2003; Minsley et al. 2012b), a similar approach that uses lateral constraints along a two-dimensional profile (Monteiro Santos 2004; Monteiro Santos et al. 2011), and smooth two-dimensional inversion approaches (e.g., Mitsuhata et al. 2006). Recent developments have also trended toward exploring multiple solutions of EC from EMI data instead of using only a single best fitting model. Examples include a two-layer, one-dimensional inversion method based on a direct-search approach that couples a global and local optimization (Mester et al. 2011) and a one-dimensional layered model estimation based on a Markov chain Monte Carlo (MCMC) approach (Minsley 2011; Minsley et al. 2012a). Section 3.1.2 includes an example of the inversion of EC made possible using this last approach (Minsley et al. 2012a).

3 EMI Instruments and Case Studies

Recent improvements in data acquisition techniques, EMI instrumentation, and inversion methods have led to unprecedented depictions of subsurface lithology and permafrost distributions from airborne electromagnetics (AEM). AEM data play a unique role in efforts to characterize permafrost over large spatial domains. The applicability in EMI for imaging physical properties at depth cannot be achieved with satellite systems, and their spatial coverage cannot be matched by ground-based measurements or borehole data. Various modalities exist for acquiring EMI data, including airborne (see Section 3.1), handheld portable (see Section 3.2 and GISCO [2014]), and cart or snowmobile towed instruments (Thiesson et al. 2009; Sudduth et al. 2001).

Increasingly, EMI measurements are being made with airborne platforms that can cover large spatial distances, particularly over remote or inaccessible terrain. One notable example where AEM was used to characterize the subsurface extent of permafrost is the recent Yukon Flats study (Minsley et al. 2012a) (discussed more in Section 3.1).

Table 3 provides cost breakdowns of AEM and human-portable systems. Section 4 is a discussion and recommendation for development of an airborne EMI capability at ERDC, but Section 3.1 provides more details on an airborne EMI system (Fugro RESOLVE system) and two human-portable systems: the Geophex GEM-2 and the Geonics EM-31. Although there are many other systems in the handheld category, such as the popular Geonics Ltd. EM-38 (Geonics Limited 2014; Sudduth et al. 2001), this report details only the GEM-2 and EM-31 as representatives of this category.

3.1 Fugro RESOLVE EMI system

AEM measurements have been used to acquire data on the electrical resistivity of materials in the subsurface below the flight path of a helicopter. The data are analyzed to interpret the subsurface lithology and the location and extent of permafrost (Figure 3). For surveys using the Fugro RESOLVE system, the electrical resistivity can be imaged to depths of approximately 50–100 m (Figures 4 and 5).

Figure 3. Airborne Electromagnetics (AEM) description (Abraham 2011).

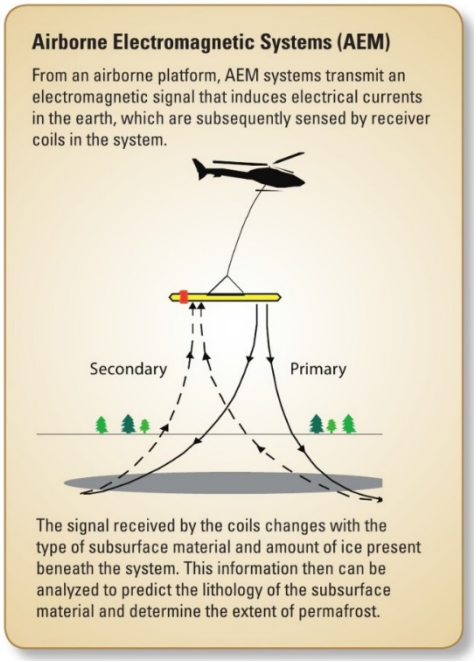

Figure 4. Three-dimensional cutout views of the resistivity model in the vicinity of (*a*) Twelvemile Lake and (*b*) the Yukon River. The gray isosurfaces are interpreted to indicate the base of permafrost in the subsurface. The upper plane in each figure is a Landsat view of the region displayed below. A talik is a region of thawed permafrost that provides a potential conduit to subsurface hydrologic flow. Vertical exaggeration is 12:1 (Minsley et al. 2012a).

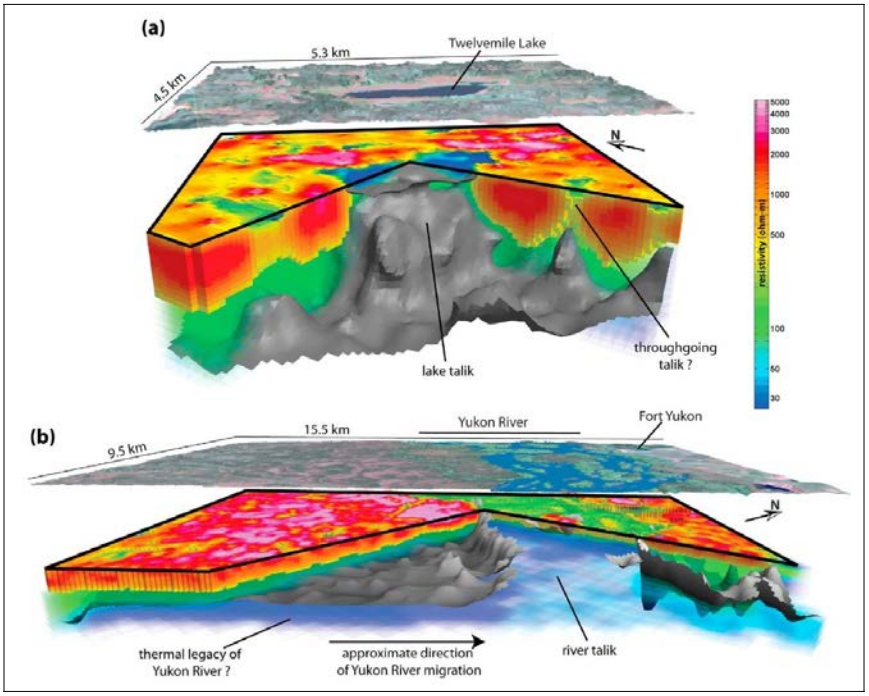

Figure 5. Resistivity cross sections along the three transects of the Fort Yukon survey. Arrows indicate the location of a sinuous side-channel of the Yukon River that is also evident as a shallow low-resistivity zone. Interpreted lithologic and permafrost boundaries are superimposed as dashed lines. Vertical exaggeration is approximately 25:1. (Minsley et al. 2012a).

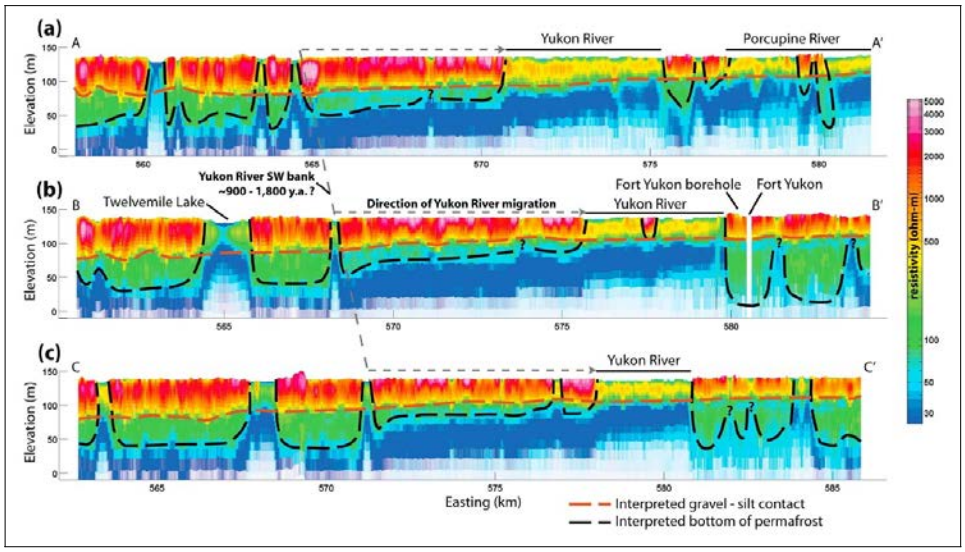

Images from these surveys can be qualitatively compared with known permafrost features and can be analyzed to identify new permafrost features. As mentioned in Section 1, electrical properties of earth materials are affected by lithology, temperature, and the presence (or absence) of ice. Of particular note is the fact that frozen materials become substantially more resistive than the same material in an unfrozen state. This allows for the identification of permafrost from the resistivity images (Abraham et al. 2011).

3.1.1 Fugro RESOLVE system specifications

This section provides a brief description of the specifications and geophysical instruments used to acquire survey data with the Fugro RESOLVE system (Figure 6). The RESOLVE system is unique, coupling horizontal coplanar coils that are capable of measuring the EM response at five frequencies by using a single coaxial coil. The approximate frequency range obtainable lies between 400 Hz and 140 kHz with the six operational frequencies logarithmically spaced (Tables 1 and 2).

Figure 6. Fugro RESOLVE system in flight (*a*) and in preparation (*b*) (Slattery and Andriashek 2012).

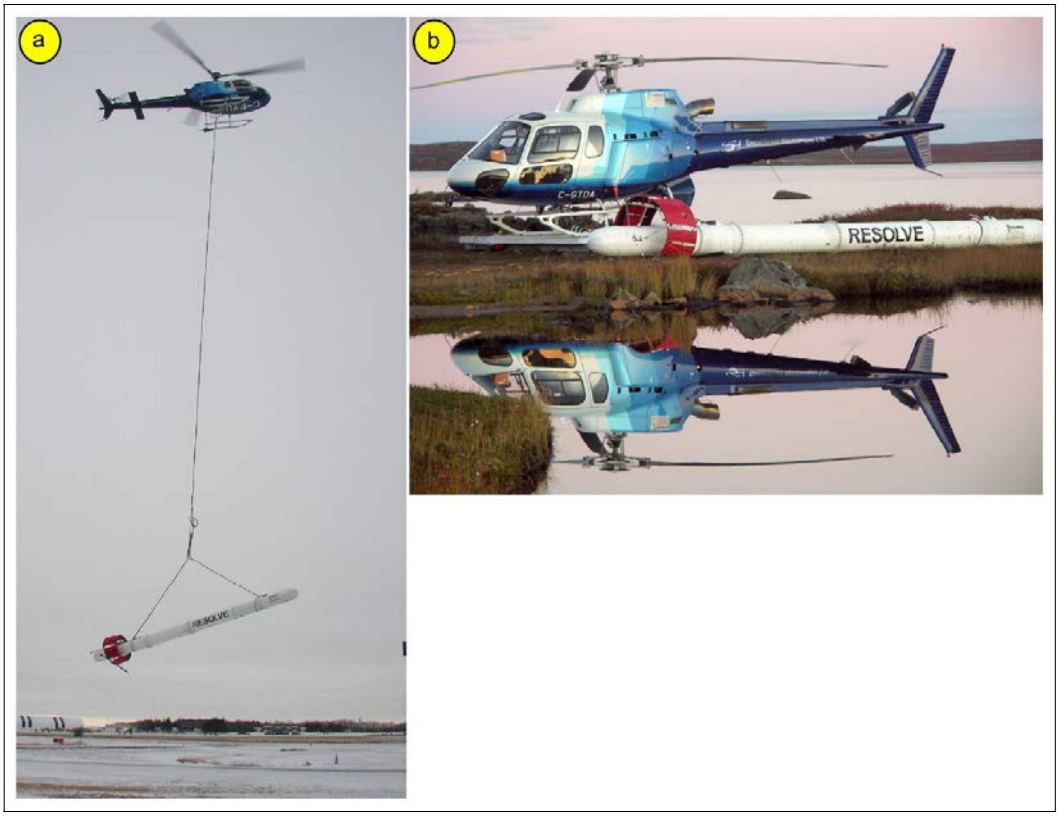

Table 1. Fugro RESOLVE system EMI specifications (Fugro Airborne Surveys 2010).

Nominal Frequency	Coil Orientation	Coil Separation (m)	Actual Running Frequency (Hz)	Channels	Sensitivity (ppm)
390 Hz	Horizontal coplanar	7.93	378	I,Q	0.12
3,300 Hz	Vertical coaxial	9.06	3260	I,Q	0.24
1,800 Hz	Horizontal coplanar	7.90	1843	I,Q	0.12
8,200 Hz	Horizontal coplanar	7.94	8180	I,Q	0.24
40,000 Hz	Horizontal coplanar	7.95	40650	I,Q	0.44
140,000 Hz	Horizontal coplanar	7.93	128510	I,Q	0.44

ppm = parts per million

Table 2. Fugro RESOLVE electromagnetic system specifications.

Coil orientations, Frequencies, and dipole moments			
Dipole Moment	Orientation	Nominal Freq. (Hz)	Actual Freq. (Hz)
310	coplanar	400	396
175	coplanar	1800	1773
211	coaxial	3300	3247
70	coplanar	8200	8220
35	coplanar	40,000	39,880
18	coplanar	140,000	132,700
Channels recorded			
6 in-phase channels 6 quadrature channels 2 monitor channels			
Sensitivity			
0.12 ppm at 400 Hz coplanar 0.12 ppm at 1800 Hz coplanar 0.12 ppm at 3300 Hz coaxial 0.24 ppm at 8200 Hz coplanar 0.60 ppm at 40,000 Hz coplanar 0.60 ppm at 140,000 Hz coplanar			
Sample Rate			
10 per second, equivalent to 1 sample every 3.3 m, at a survey speed of 120 km/h			

The multi-coil coaxial/coplanar technique energizes conductors in different directions. The coaxial coils are vertical with their axes in the flight direction, and the coplanar coils are horizontal. The secondary fields are sensed simultaneously by means of receiver coils that are maximally coupled to their respective transmitter coils. The system yields an in-phase and a quadrature channel from each transmitter–receiver coil pair.

The Fugro RESOLVE system is frequently installed in Airbus Helicopters (manufactured in Marignane, France), models AS350-B2 or AS350-B3 single-engine helicopters. These aircraft provide a safe and efficient platform for EMI surveys. The system is towed in a symmetric dipole configuration operated at a nominal survey altitude of 30 m. Coil separation is 7.9 m for 400 Hz, 1800 Hz, 8200 Hz, 40,000 Hz, and 140,000 Hz and 9.0 m for the 3300 Hz coil pair (Slattery and Andriashek 2012). During flight, the helicopter is typically flown at 120 km/h 60 m above the ground

level while the RESOLVE boom is suspended 30 m above the ground (Cain 2004).

The apparent resistivities in $\Omega \cdot m$ are generated from the in-phase and quadrature EM components for all of the coplanar frequencies by using a pseudo-layer half-space model. The inputs to the resistivity algorithm are the in-phase and quadrature amplitudes of the secondary field. The algorithm calculates the apparent resistivity in $\Omega \cdot m$ and the apparent height of the bird above the conductive source. Other more sophisticated models have also been used (Minsley et al. 2012a) to produce the results described in Section 3.1.2.

The RESOLVE system carries other instruments to aid in data acquisition and processing. These instruments include an airborne magnetometer, an airborne GPS (global positioning system) receiver, a radar altimeter, barometric pressure and temperature sensors, a laser altimeter, a proprietary digital data-acquisition system, and a flight-path video-recording system. For more information on these auxiliary instruments and for results of Fugro RESOLVE surveys, see Cain (2004), Fugro Airborne Surveys (2010), and Slattery and Andriashek (2012). Figures 7 and 8 illustrate the data processing flow and the coil arrangement for the FUGRO system.

Figure 7. Fugro RESOLVE electromagnetic data flowchart (Slattery and Andriashek 2012).

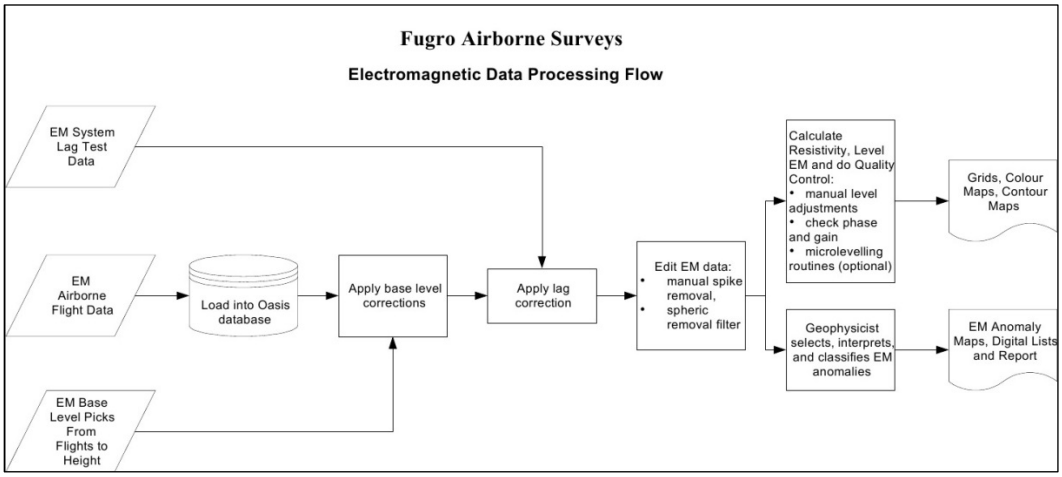

Figure 8. Fugro RESOLVE coil layout.

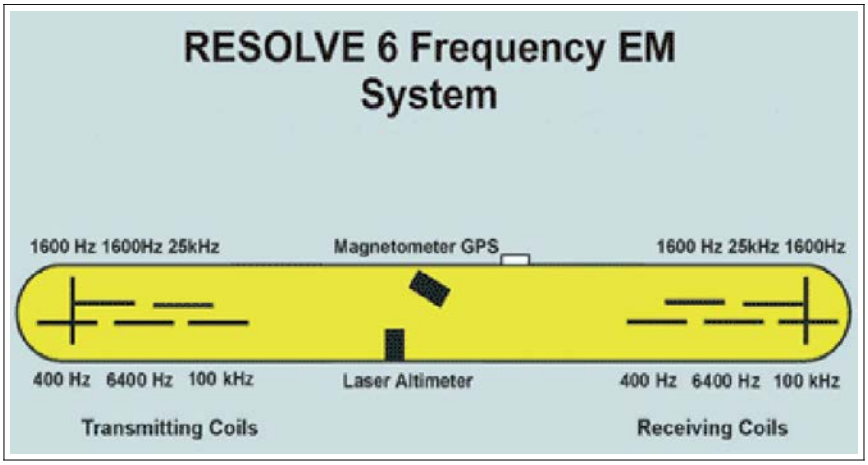

3.1.2 Fugro RESOLVE survey at Fort Yukon, AK

The U.S. Geological Survey (USGS) conducted the Fort Yukon survey in 2010 to detect resistivity contrasts in and around the Fort Yukon area and to evaluate the effectiveness of using frequency domain electromagnetics to map permafrost.

The Yukon Flats is a lowland area within the Yukon River Basin where the Yukon River reaches its northernmost point approximately 13 km north of the Arctic Circle (66.66° N). The Yukon Flats is of particular importance because it is underlain by discontinuous permafrost that is generally more unstable and more sensitive to a warming climate when compared to continuous permafrost. Because discontinuous permafrost is relatively warm (i.e., −1°C or −2°C), contact with and heat transfer from adjacent unfrozen ground or surface and subsurface water bodies can result in significant thawing (Minsley et al. 2012a).

USGS acquired AEM data during one week in June 2010 by using the Fugro RESOLVE system operating at six frequencies between 0.4 and 129 kHz and flown at an average speed of 30 m/s and a vertical ground clearance of 30 m. The survey consisted of a block of lines spaced 350 m apart, covering an area approximately 300 km^2, and a number of widely spaced "reconnaissance" lines, totaling nearly 900 km in length, that represented a broad range of geologic features within the Yukon Flats area (Fugro Airborne Surveys 2010). High-resolution mapping in three dimensions was achieved within the block, and visualization of different hydrogeologic settings and permafrost distributions along the widely spaced lines provided

new understanding of the Yukon Flats at both small (10s of meters) and large (kilometers) scales. Inversion of approximately 500,000 AEM soundings yielded densely sampled models of electrical resistivity along the survey flight lines to depths of about 100 m (Minsley et al. 2012a).

Results from this study and others (such as work near Alberta, Canada) (Slattery and Andriashek 2012) highlight the need for detailed and large-scale conductivity mapping to survey permafrost regions in Alaska. Because of the prohibitive costs of these AEM surveys ($100K just to mobilize), ERDC and others desire alternatives that can map smaller areas by using fewer resources and in a more flexible manner (see Section 4).

3.2 Geophex GEM-2 system

The GEM-2 is a fixed-geometry EMI instrument designed to be carried by a single person to make electrical conductivity measurements. It is a hand-held, digital, multi-frequency sensor. The GEM-2 operates in a frequency range of about 300 Hz to 96 kHz and can transmit an arbitrary waveform containing multiple frequencies. The unit is capable of transmitting and receiving any digitally synthesized waveform by means of the pulse-width modulation technique. Owing to the arbitrary nature of its broadcast waveform and high-speed digitization, the sensor can operate either in a frequency-domain mode or in a time-domain mode.

Figure 9 shows the most recent portable version of GEM-2. The sensor weighs about 4 kg, and the built-in operating software allows a surveyor to cover roughly one acre per hour at a line spacing of 1.5 m. Along a survey line, the data rate is about two every 30 cm, resulting in about 20,000 data points per acre per hour.

Figure 9. Geophex GEM-2 sensor in various modes of operation (Geophex Ltd. 2014).

Figure 10 shows the electronic block diagram of GEM-2. The sensor contains a transmitter coil and a receiver coil that are separated by about 1.7 m. Such geometry is called a bistatic configuration. It also contains a third bucking coil that removes (or bucks) the primary field from the receiver coil. All coils are molded into a single board (a ski) in a fixed geometry, rendering a light and portable package. A removable signal-processing console is attached to the ski.

Figure 10. Geophex GEM-2 sensor block diagram (Geophex Ltd. 2014).

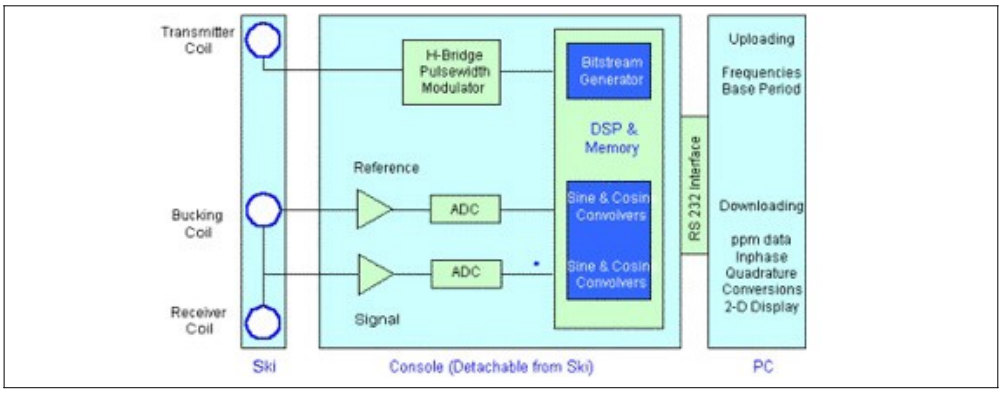

Figure 11 shows data from the GEM-2 locating a buried pipe. This figure shows the GEM-2 in-phase response at 7290 Hz over a known stainless-steel pipe 45 cm in diameter, buried at a depth of approximately 9 m. A magnetic survey failed to detect the pipe, presumably because it is made of stainless steel, a non-ferrous metal. In this example, the plot showing the ppm response is sufficient to locate the pipe. The survey over this pipe included seven frequencies, and the response was highly dependent on frequency. For example, the pipe was not recognizable at around 2 kHz or 12 kHz.

Figure 11. Geophex GEM-2 sensor data over a stainless steel pipe buried at approximately 9 m (Geophex Ltd. 2014).

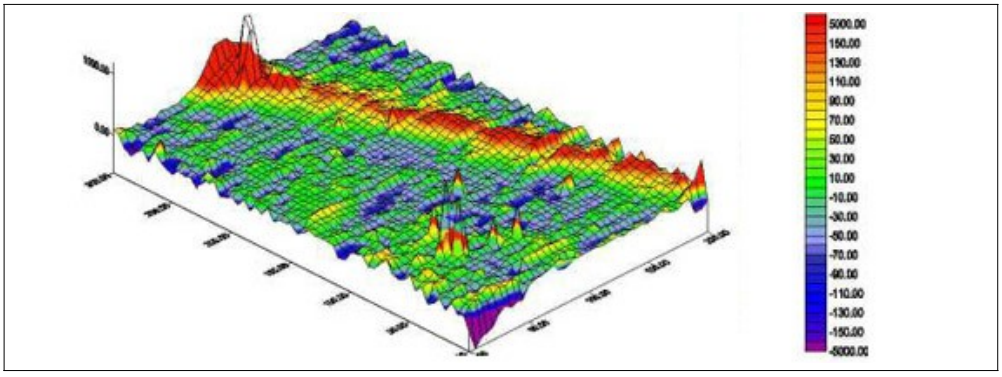

3.3 Geonics EM-31

The EM-31 is a single-frequency EMI instrument made by Geonics that maps ground conductivity. Surveys can be carried out under most geological conditions, including those of high surface resistivity, such as sand, gravel, and asphalt. The effective depth of exploration is about 6 m, making it suitable for shallow permafrost-detection surveys. The EM-31-MK2 is an updated version of the standard EM-31 with the data logger now incorporated into the control console. ERDC owns three EM-31 units (see Figure 12 and Section 4), and Bjella et al. (2010) document their field use.

Figure 12. *Upper*: Geonics EM-31 EMI sensor owned by ERDC. *Lower*: EM-31 conductivity survey of a test area including buried test items at Fort Wainwright, AK (Bjella et al. 2010).

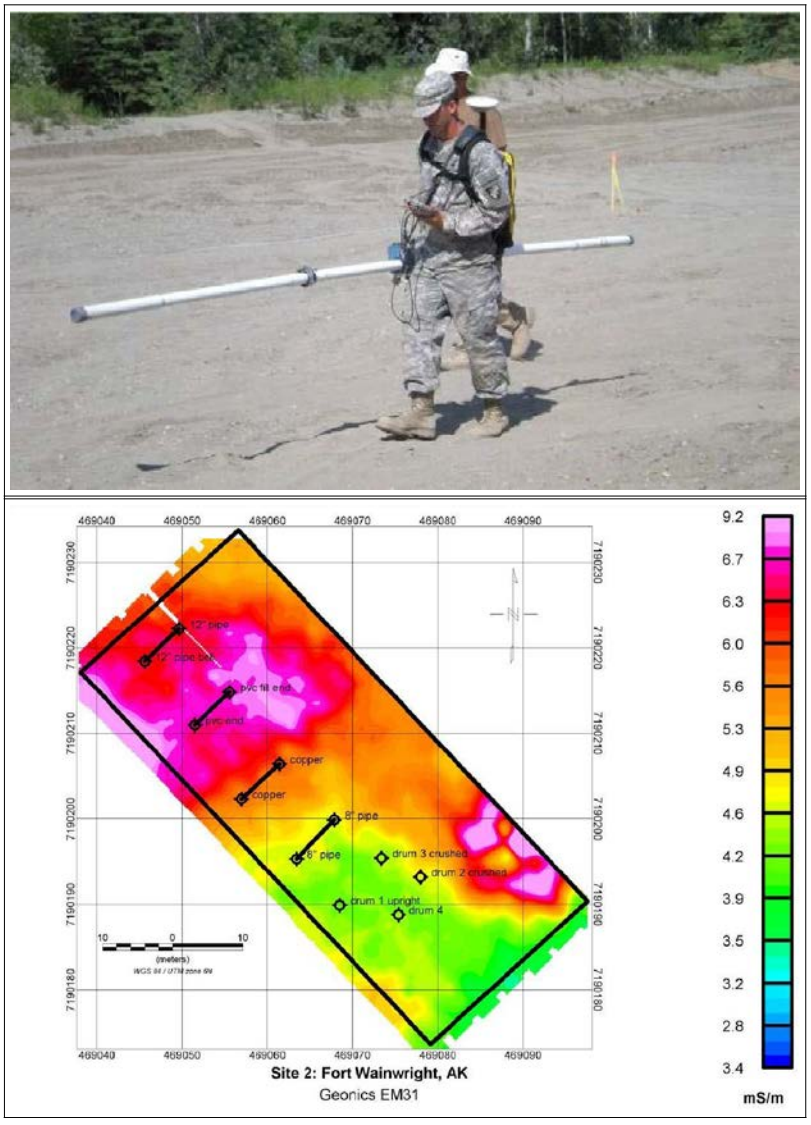

3.4 Comparison of survey methods

Commercial EMI instruments currently are able to measure subsurface conductivity by using a variety of modalities. Table 3 compares and summarizes various aspects of these system, including a conceptual unmanned helicopter-based system described in Section 5.

Table 3. A comparison of EMI survey modalities.

System Name	Modality	Operational Frequencies	Depth	Initial Cost	Ongoing Cost	Linear Resolution	ERDC Owned?
GEM-2	handheld	330 Hz–96 kHz	2 m	$20K	8 acres / person / day	15 cm	yes
EM-31	handheld	9.8 kHz	6 m	$15K	12 acres / person / day	50 cm	yes
EM-31 towed	towed	9.8 kHz	7 m	$15K	60 acres / person / day + equipment	2.5 m	yes
Fugro RESOLVE	helicopter	400 Hz–140 kHz	100 m	$100K to mobilize	very high	3.3 m	no
ERDC UEMI	UAV	500 Hz–100 kHz	25 m	R&D	one person	1 m	concept

UAV = unmanned aerial vehicle

R&D = research and development

4 ERDC EMI Sensing Capabilities

ERDC researchers have been making conductivity measurements in permafrost terrains since the 1970s (Arcone et al. 1979; Osterkamp et al. 1980). For example, the ERDC Geotechnical and Structures Laboratory (GSL) has been doing this type of work since the 1980s.

Recently, ERDC teams have performed numerous conductivity surveys on permafrost terrains in the Fairbanks, AK, area with a focus on ground-state investigations supporting potential military construction sites (Bjella et al. 2010).

As of the writing of this report, ERDC owns the following ground-based instruments capable of measuring the conductivity of soils and permafrost:

- EMI Instruments
  - Geonics EM38
  - Geonics EM38B
  - Geonics EM38-MK2 (3 units)
  - Geonics EM-31 (3 units)
  - Geonics EM34XL
  - Geonics ProTEM47
  - Geophex GEM-2
  - Geophex GEM-2H
- Capacitively Coupled Resistivity
  - Geometrics OhmMapper (2 units)
- Galvanic Contact Resistivity
  - AGI SuperSting R8 Electrical Resistivity System 112 electrodes
  - AGI SuperSting R8 Electrical Resistivity System 84 electrodes

Ben Barrowes at the ERDC Cold Regions Research Engineering Laboratory (CRREL) and Fridon Shubitidze at Dartmouth College lead a research group that has constructed several research-grade EMI instruments. These projects, funded by the Department of Defense's Strategic Environmental Research and Development Program (SERDP), include the Man-Portable Vector instrument (Fernández et al. 2011a,2011b; Barrowes et al. 2009; Barrowes 2012) (SERDP# MR-1443, see Figure 13a), the GEM-3D + (O'Neill 2005; Fernández et al. 2009; Barrowes 2011) (SERDP# MR-1537,

see Figure 13b), and the Pedemis Instrument (Barrowes et al. 2012a, 2012b, 2013a, 2013b; Grzegorczyk and Barrowes 2014; Shubitidze et al. 2012) (SERDP# MR-1712, see Figure 13c). These instruments were constructed to detect and classify UXO, but they could be used to extract shallow EC estimates similar to in Huang and Won (2003).

Figure 13. EMI research instruments developed under SERDP-funded projects at CRREL and Dartmouth.

(a) Man-Portable Vector instrument, SERDP# MR-1443

(b) GEM-3D +sensor, SERDP# MR-1537

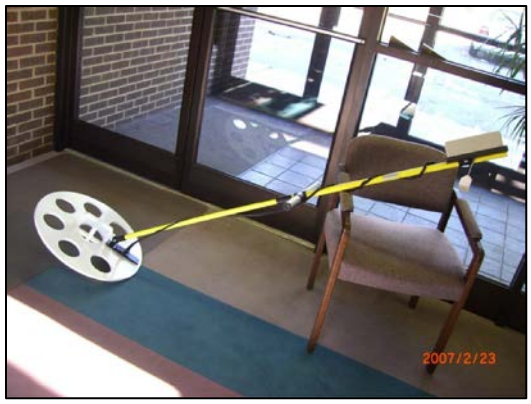

(c) Pedemis Instrument, SERDP# MR-1712

5 Discussion and Proposed Development of a Conceptual EMI EC Instrument

ERDC has both the field and research expertise to acquire EMI measurements and to extract electrical conductivity values from those measurements. ERDC also owns several different types of commercial and research-grade EMI instruments. For smaller areas and depths of investigation, ERDC can map EC up to 6 m deep at the rate of one acre per hour by one person using the EM-31. ERDC currently has no in-house capability using EMI methods to map EC beyond 6 m deep or at acquisition rates similar to the Fugro RESOLVE system.

ERDC has an opportunity to develop a compromise between these two ends of the spectrum. This compromise could consist of either using existing in-house systems or developing a novel system and using the instrument in a new modality. For example, an existing instrument such as the EM-31 could be used in a new modality by dragging it behind a human-operated snowmobile or an autonomous vehicle. Data from the EM-31 acquired at this nonstandard height would be interpreted in-house by Barrowes' research group to obtain EC over lines or areas.

Another possibility is to use unmanned helicopters to acquire data over larger areas. Drone helicopters such as the Yamaha RMax (Yamaha 2013) (see Figure 14) have maximum payloads of 28 kg, a flying time of 45–60 min, and a maximum speed of 40 km/hr. The stock RMax would need to be modified to incorporate GPS and other sensors similar to what the BEAR (Berkley Aerial Robots) project has done (Figure 15) (Berkley Aerobot Team 2005).

The RMax could handle a larger instrument than the EM-31. An instrument developed within ERDC using expertise developed under the SERDP projects listed above could result in a multi-frequency, multi-coil system similar to the RESOLVE system but at about half the size. This system would cost only a fraction of what other helicopter-based platforms require for operation. As a conceptual design, this new instrument could be roughly 6–7 m long. The boom could be suspended 1 m above the ground with the RMax 6–11 m above the ground, resulting in a depth of investiga-

tion of about 20–25 m. Assuming a 50% flight duty cycle, in 8 hr, this instrument on an unmanned helicopter could potentially survey a 160 km long line, or approximately 3 km^2 per day, assuming a 20 m line spacing. See Table 2 for a comparison of this conceptual system to other EMI systems.

Figure 14. Yamaha RMax unmanned helicopter with a maximum payload of 28 kg, a flying time of 45–60 min, and a maximum speed of 40 km/hr (Yamaha 2013).

Figure 15. Berkeley BEAR Fleet: Ursa Maxima 1 additional instruments (Berkley Aerobot Team 2005).

Instead of a rigid boom containing coils and instrumentation, some EMI systems, like the EM34 from Geonics (Monteiro Santos 2004), consist of separated, physically decoupled coils (Figure 16). Following this concept, another modality for a new instrument could be a swarm of smaller, lighter drones not physically connected (see the drone swarm concept in Figure 17).

Figure 16. Geonics EM34 showing physically decoupled transmitter and receiver coils (Geonics Limited 2013).

Figure 17. Possible drone swarm concept (MedFlight 2014).

In this configuration, one or more drone would carry transmitters; and several other drones would carry receivers. This would greatly reduce the payload of any one drone and, therefore, would dramatically reduce drone size and cost. Two main problems would arise for a drone swarm:

- Communication between drones would add to the initial design complexity.
- It would require positioning the transmitter to a level that allows sufficient background subtraction.

Positioning the transmitter drone could potentially be accomplished using a beacon approach (Lhomme et al. 2011; Fernández et al. 2009), which uses the primary field itself to locate the transmitter, or perhaps by real time video from each receiver drone.

A drone-helicopter- or drone-swarm-based system as described here could enable many applications, not just EC surveys focusing on permafrost. Other EC features could also be mapped (see Section 2.2), and applications such as tunnel detection, dangerous- or denied-area surveys, border crossing monitoring, etc., could be enabled on the same platform. In fact, most applications of EMI technologies where remote sites, environmental hazards, rough terrain, or conflict zones are common could be locales that could use an airborne EMI sensor. For example, the detection of UXOs on impact areas where human travel is not possible or for surveys over rough landscape surfaces where walking, towing, or dragging EMI equipment is not feasible would benefit from airborne sensors. Further, if the EMI equipment can be reduced to an even smaller payload and volumetric size, the equipment could then be deployed to identify buried mines or to search for underground tunnels or bunkers in conflict locations.

6 Conclusion

Arctic environments have garnered substantial interest because of their susceptibility to climate change and increasing availability of resources. Of particular concern is the design and siting of horizontal and linear infrastructure on permafrost. Permafrost is ubiquitous in cold regions; but the details of its distribution, particularly at depth, remain largely unknown. An added challenge for infrastructure development in permafrost terrains is that projected climate warming will lead to degradation of subsurface permafrost bodies. Currently, tools for identifying and mapping permafrost structure and geomorphology in the subsurface are limited. Many of the current tools require vehicle access or can survey only a kilometer or two in a single day.

The EMI method is advantageous for characterizing shallow, subsurface systems when compared with other methods because large areas can be traversed in a minimal amount of time and in a noninvasive manner. Airborne platforms have the potential to provide a system that can map permafrost terrains during all seasons and in remote, inaccessible, and denied areas.

ERDC has an in-house EMI capability that includes both field and research expertise. Potential development opportunities exist to either automate existing instruments with the use of robots or drones or to develop a new instrument to be flown on an unmanned helicopter.

The use of robotic and autonomous systems is becoming more widespread in many fields of research, including in geophysics. Medium-scale systems composed of instruments that measure the electrical conductivity of the subsurface have the potential to enable safer and larger-scale EC surveys for less cost than large-scale or ground-based systems. EC measurements to determine permafrost state and other parameters of the subsurface will enable better decisions regarding planning and infrastructure than currently possible.

References

Abraham, J. 2011. *A Promising Tool for Subsurface Permafrost Mapping: An Application of Airborne Geophysics from the Yukon River Basin, Alaska*. Fact Sheet 2011-3133. Reston, VA: U.S. Geological Survey.

Abraham, J., L. Ball, J. Cannia, T. Jorgenson, B. Minsley, B. Smith, M. Walvoord, B. Wylie, and C. Voss. 2011. Airborne Electromagnetic Mapping of Subsurface Permafrost-Quantifiable Characterization for Now and in the Future. In *Proceedings of the 6th International Conference on Arctic Margins, Fairbanks, AK, May 30–June 3*.

Allen, D. 2007. *Irrigation Insights 7—Geophysics for the Irrigation Industry*. Canberra, Australia: Land and Water Australia.

Allred, B., M. R. Ehsani, and D. Saraswat. 2006. Comparison of Electromagnetic Induction, Capacitively-Coupled Resistivity, and Galvanic Contact Resistivity Methods for Soil Electrical Conductivity Measurement. *Applied Engineering in Agriculture*. 22 (2): 215–230.

Ao, C. O. 2001. Electromagnetic Wave Scattering by Discrete Random Media with Remote Sensing Applications. PhD thesis, Massachusetts Institute of Technology.

Arcone, S., P. Sellmann, and A. Delaney. 1979. *Effects of Seasonal Changes and Ground Ice on Electromagnetic Surveys of Permafrost*. CRREL Report 79-23. Hanover, NH: U.S. Army Cold Regions Research and Engineering Laboratory.

Auken, E., L. Pellerin, N. B. Christensen, and K. Srensen. 2006. A Survey of Current Trends in Near-Surface Electrical and Electromagnetic Methods. *Geophysics* 71 (5): G249–G260.

Barrowes, B. E. 2004. Electromagnetic scattering and Induction Models for Spheroidal Geometries. PhD thesis, Massachusetts Institute of Technology.

———. 2011. *Handheld Frequency Domain Vector EMI Sensing for UXO Discrimination*. SERDP MM1537 Final Annual Report. Alexandria, VA: Strategic Environmental Research and Development Program (SERDP).

———. 2012. *Man-Portable Vector Time Domain EMI Sensor and Discrimination Processing*. SERDP MM1443-FY06 annual report. Alexandria, Virginia: Strategic Environmental Research and Development Program (SERDP).

Barrowes, B. E., F. Shubitidze, P. Fernández, I. Shamatava, and K. O'Neill. 2009. *Man-Portable Vector EMI Instrument Data Characterization Using the NSMS Method*. In *Proceedings of SPIE 0303*. Bellingham, WA: SPIE

Barrowes, B. E., F. Shubitidze, J. P. Fernández, T. M. Grzegorczyk, and K. O'Neill. 2012a. Pedemis: A Portable Electromagnetic Induction Sensor with Integrated Positioning. In *Proceedings of SPIE 8375, Detection and Sensing of Mines, Explosive Objects, and Obscured Targets XVII, 27 April*, ed. J. T. Broach, and J.T. Holloway Jr. Bellingham, WA: SPIE.

Barrowes, B. E., F. Shubitidze, T. M. Grzegorczyk, P. Fernández, and K. ONeill. 2012b. Electromagnetic Induction Sensing of Unexploded Ordnance with Pedemis. In *Proceedings of the Joint Meeting of the Military Sensing Symposia (MSS), Washington, DC, 22–25 October*.

Barrowes, B. E., T. M. Grzegorczyk. F. Shibitidze, P. Fernández, and K. O'Neill. 2013a. The Pedemis Instrument: Operation and APG Field Results. In *Procedings of SPIE 8709, Detection and Sensing of Mines, Explosive Objects, and Obscured Targets XVIII, 7 June*, ed. J. T. Broach. Bellingham, WA: SPIE. doi:10.1117/12.2014964.

Barrowes, B. E., F. Shubitidze, T. M. Grzegorczyk, J. P. Fernández, and K. O'Neill. 2013b. The Pedemis Instrument: Positioning, Background Subtraction, and APG Field Results. In *Proceedings of SPIE 8709, Detection and Sensing of Mines, Explosive Objects, and Obscured Targets XVIII, 7 June*, ed. J. T. Broach. Bellingham, WA: SPIE.

Berkeley Aerobot Team. 2005. Testbeds and Experiment Facility. BEAR: Berkeley Aerobot Team. https://robotics.eecs.berkeley.edu/bear/acclimate/acclimate2005_david.ppt (accessed 27 August 2014).

Bjella, K. L., B. N. Astley, and R. E. North. 2010. *Geophysics for Military Construction Projects*. ERDC TR-10-9. Hanover, NH: U.S. Army Research and Development Center.

Cain, M. J. 2004. *Resolve Survey for U. S. Geological Survey*. Technical Report #04034 for the United States Geological Survey. Ontario, Canada: Fugro Airborne Surveys.

Chapman, W. L., and J. E. Walsh. 2007. Simulations of Arctic Temperature and Pressure by Global Coupled Models. *Journal of Climate* 20 (4): 609–632.

Corwin, D., and S. Lesch. 2005. Apparent Soil Electrical Conductivity Measurements in Agriculture. *Computers and Electronics in Agriculture* 46 (1–3): 11–43.

Corwin, D., and R. Plant. 2005. Applications of Apparent Soil Electrical Conductivity in Precision Agriculture. *Computers and Electronics in Agriculture* 46 (1–3): 1–10.

Dafflon, B., S. S. Hubbard, C. Ulrich, and J. E. Peterson. 2013. Electrical Conductivity Imaging of Active Layer and Permafrost in an Arctic Ecosystem, Through Advanced Inversion of Electromagnetic Induction Data. *Vadose Zone Journal* 12 (4).

Farquharson, C. 2000. *EM1DFM: A Program Library for Forward Modelling and Inversion of Frequency Domain Electromagnetic Data over 1D Structures, Version 1.0*. Technical Report. Vancouver, British Columbia: University of British Columbia, Geophysical Inversion Facility, Department of Earth and Ocean Sciences.

Fernández, J., B. Barrowes, K. O'Neill, I. Shamatava, and F. Shubitidze. 2009. A Vector Handheld Frequency-Domain Sensor for UXO Identification. In *Proceedings of the SPIE 7303, Detection and Sensing of Mines, Explosive Objects, and Obscured Targets XIV*, ed. R. S. Harmon, J. T. Broach, J. H. Holloway Jr. Bellingham, WA: SPIE.

Fernández, J. P., B. E. Barrowes, T. M. Grzegorczyk, N. Lhomme, K. O'Neill, and F. Shubitidze. 2011a. A Man-Portable Vector Sensor for Identification of Unexploded Ordnance. *IEEE Sensors Journal* 11:2542–2555.

Fernández, J. P., B. E. Barrowes, N. Lhomme, A. Bijamov, T. Grzegorczyk, K. O'Neill, I. Shamatava, and F. Shubitidze. 2011b. MPV-II: An Enhanced Vector Man-Portable EMI Sensor for UXO Identification. In *Proceedings of SPIE 8017, Detection and Sensing of Mines, Explosive Objects, and Obscured Targets XVI*, ed. R. S. Harmon, J. H. Holloway, Jr., and J. T. Broach. Bellingham, WA: SPIE.

Fraser, D. C. 1978. Resistivity Mapping with an Airborne Multicoil Electromagnetic System. *Geophysics* 43 (1): 144–172.

Fugro Airborne Surveys. 2010. *Logistics and Processing Report Airborne Magnetic and RESOLVE Survey*. Job No. 10026 and 10039. Technical report for the United States Geological Survey. Ontario, Canada: Fugro Airborne Surveys.

Geonics Limited. 2013. EM34-3 | EM34-3XL. Ontario, Canada: Geonics Limited. http://www.geonics.com/html/em34-3.html (accessed 21 August 2014).

———. 2014. EM38-MK2. Ontario, Canada: Geonics Limited. http://www.geonics.com/html/em38.html (accessed 21 August 2014).

Geophex Ltd. 2014. Geophex Electromagnetic Sensors. Geophex Ltd. http://www.geophex.com/Pubs/gem2_-_how_it_works_detailed.htm (accessed 21 August 2014).

GISCO. 2014. CMD EM Ground Conductivity Meters. Minneapolis, MN: GISCO. http://www.giscogeo.com/pages/emgycm. html (accessed 21 August 2014).

Grzegorczyk, T. M., and B. E. Barrowes. 2014. Operation of the Pedemis Sensor at the Aberdeen Proving Ground Standardized Test Site: Single and Multi-Target Inversions. *IEEE Geoscience and Remote Sensing Letters* 11 (2): 394–398. doi: 10.1109/LGRS.2013.2263333. http://ieeexplore.ieee.org/stamp/stamp.jsp?tp=&arnumber=6529113&isnumber=6675034.

Hauck, C., and C. Kneisel, ed. 2008. *Applied Geophysics in Periglacial Environments*. Cambridge, UK: Cambridge University Press.

Hendrickx, J., B. Borchers, D. Corwin, S. Lesch, A. Hilgendorf, and J. Schlue. 2002. Inversion of Soil Conductivity Profiles from Electromagnetic Induction Measurements. *Soil Science Society of America Journal* 66 (3): 673–685.

Hoekstra, P., P. Sellmann, and A. Delaney. 1975. Ground and Airborne Resistivity Surveys of Permafrost near Fairbanks, Alaska. *Geophysics* 40 (4): 641–656.

Huang, H., and D. C. Fraser. 2000. Airborne Resistivity and Susceptibility Mapping in Magnetically Polarizable Areas. *Geophysics* 65 (2): 502–511.

———. 2003. Inversion of Helicopter Electromagnetic Data to a Magnetic Conductive Layered Earth. *Geophysics* 68 (4): 1211–1223.

Huang, H., and I. Won. 2003. Real-Time Resistivity Sounding Using a Hand-Held Broadband Electro-Magnetic Sensor. *Geophysics* 68 (4): 1224–1231.

Kuras, O., D. Beamish, P. I. Meldrum, and R. D. Ogilvy. 2006. Fundamentals of the Capacitive Resistivity Technique. *Geophysics* 71 (3): G135–G152.

Lhomme, N., B. E. Barrowes, and D. C. George. 2011. EMI Sensor Positioning Using a Beacon Approach. In *Proceedings of SPIE 8017, Detection and Sensing of Mines, Explosive Objects, and Obscured Targets XVI*, ed. R. S. Harmon, J. Holloway Jr., and J. T. Broach. Bellingham, WA: SPIE.

MedFlight, A. 2014. Drone Swarm. *Angel MedFlight Blog*. http://blog.angelmedflight.com/2014/03/17/drone-swarm/ (accessed 7 November 2014).

Mester, A., J. van der Kruk, E. Zimmermann, and H. Vereecken. 2011. Quantitative Two-Layer Conductivity Inversion of Multi-Configuration Electromagnetic Induction Measurements. *Vadose Zone Journal* 10 (4): 1319–1330.

Minsley, B. J. 2011. A Trans-Dimensional Bayesian Markov Chain Monte Carlo Algorithm for Model Assessment Using Frequency-Domain Electromagnetic Data. *Geophysical Journal International* 187 (1): 252–272.

Minsley, B. J., J. D. Abraham, B. D. Smith, J. C. Cannia, C. I. Voss, M. T. Jorgenson, M. A. Walvoord, B. K. Wylie, L. Anderson, L. B. Ball, M. Deszcz-Pan, T. P. Wellman, and T. A. Ager. 2012a. Airborne Electromagnetic Imaging of Discontinuous Permafrost. *Geophysical Research Letters* 39 (2): L02503.

Minsley, B. J., B. D. Smith, R. Hammack, J. L. Sams, and G. Veloski. 2012b. Calibration and Filtering Strategies for Frequency Domain Electromagnetic Data. *Journal of Applied Geophysics* 80:56–66.

Mitsuhata, Y., T. Uchida, K. Matsuo, A. Marui, and K. Kusunose, 2006. Various-Scale Electro-Magnetic Investigations of High-Salinity Zones in a Coastal Plain. *Geophysics* 71 (6): B167–B173.

Monteiro Santos, F. A. 2004. 1-D Laterally Constrained Inversion of EM34 Profiling Data. *Journal of Applied Geophysics* 56 (2): 123–134.

Monteiro Santos, F. A., J. Triantafilis, and K. Bruzgulis. 2011. A Spatially Constrained 1D Inversion Algorithm for Quasi-3D Conductivity Imaging: Application to Dualem-421 Data Collected in a Riverine Plain. *Geophysics* 76 (2): B43–B53.

O'Neill, K. 2005. *The GEM-3D.* SEED #1353. Alexandria, VA: Strategic Environmental Research and Development Program (SERDP).

Osterkamp, T. E., R. Jurick, G. Gislason, and S. I. Akasofu. 1980. Electrical Resistivity Measurements in Permafrost Terrain at the Engineer Creek Road Cut, Fairbanks, Alaska. *Cold Regions Science and Technology* 3 (4): 277–286.

Overduin, P. P., S. Westermann, K. Yoshikawa, T. Haberlau, V. Romanovsky, and S. Wetterich. 2012. Geoelectric Observations of the Degradation of Nearshore Submarine Permafrost at Barrow (Alaskan Beaufort Sea). *Journal of Geophysical Research: Earth Surface (2003–2012)* 117 (F2).

Racine, C. H., and J. C. Walters. 1994. Groundwater-Discharge Fens in the Tanana Lowlands, Interior Alaska, U.S.A. *Arctic and Alpine Research* 26 (4): 418–426.

Reynolds, J. M. 2011. *An Introduction to Applied and Environmental Geophysics*. Hoboken, NJ: John Wiley & Sons.

Sharma, P. V. 1997. *Environmental and Engineering Geophysics*. Cambridge University Press.

Shubitidze, F., I. Shamatava, J. Fernández, B. Barrowes, K. O'Neill, and A. Bijamov. 2012. ONVMS Applied to a New Advanced Portable EMI System Data. In *Proceedings of the 2012 XVIIth International Seminar/Workshop on Direct and Inverse Problems of Electromagnetic and Acoustic Wave Theory (DIPED), 24–27 September, Tbilisi, Georgia*, 145–148.

Slattery, S., and L. Andriashek. 2012. *Overview of Airborne-Electromagnetic and -Magnetic Geo-Physical Data Collection Using the RESOLVE and GEOTEM Surveys near Red Deer, Central Alberta*. ERCB/AGS Open File Report 2012-07. Alberta, Canada: Energy Resources Conservation Board, Alberta Geological Survey.

Sudduth, K., S. Drummond, and N. Kitchen, 2001. Accuracy Issues in Electromagnetic Induction Sensing of Soil Electrical Conductivity for Precision Agriculture. *Computers and Electronics in Agriculture* 31 (3): 239–264.

Thiesson, J., M. Dabas, and S. Flageul. 2009. Detection of Resistive Features Using Towed Slingram Electromagnetic Induction Instruments. *Archaeological Prospection* 16 (2): 103–109. doi:10.1002/arp.350.

U.S. EPA (U.S. Environmental Protection Agency). 2014a. Geophysical Methods. Environmental Geophysics. Washington, DC: U.S. Environmental Protection Agency. http://water.usgs.gov/ogw/bgas/methods.html (accessed 21 August 2014).

———. 2014b. Resistivity Methods. Environmental Geophysics. Washington, DC: U.S. Environmental Protection Agency. http://pubs.usgs.gov/sir/2005/5205/ (accessed 21 August 2014).

Walker, M. D., C. H. Wahren, R. D. Hollister, G. H. Henry, L. E. Ahlquist, J. M. Alatalo, M. S. Bret-Harte, M. P. Calef, T. V. Callaghan, A. B. Carroll, et al. 2006. Plant Community Responses to Experimental Warming Across the Tundra Biome. In *Proceedings of the National Academy of Sciences of the United States of America* 103 (5): 1342–1346.

Ward, S. H., and G. W. Hohmann. 1988. Electromagnetic Theory for Geophysical Applications. In *Electromagnetic Methods in Applied Geophysics* 1:130–311. Tulsa, OK: Society of Exploration Geophysicists.

Wolken, J. M., T. N. Hollingsworth, T. S. Rupp, F. S. Chapin III, S. F. Trainor,T. M. Barrett,P. F. Sullivan, A. D. McGuire, E. S. Euskirchen, P. E. Hennon, et al. 2011. Evidence and Implications of Recent and Projected Climate Change in Alaska's Forest Ecosystems. *Ecosphere* 2 (11): art124.

Yamaha. 2013. Yamaha RMAX Specifications. Yamaha Motor Australia. http://rmax.yamaha-motor.com.au/specifications (accessed 27 August 2014).

Yoshikawa, K., V. Romanovsky, N. Duxbury, J. Brown, and A. Tsapin. 2004. The Use of Geophysical Methods to Discriminate Between Brine Layers and Freshwater Taliks in Permafrost Regions. *Journal of Glaciology and Geocryology* 26:301–309.

Zhang, T., O. W. Frauenfeld, M. C. Serreze, A. Etringer, C. Oelke, J. McCreight, R. G. Barry, D. Gilichinsky, D. Yang, H. Ye, et al. 2005. Spatial and Temporal Variability in Active Layer Thickness over the Russian Arctic Drainage Basin. *Journal of Geophysical Research: Atmospheres (1984–2012)* 110(D16).

REPORT DOCUMENTATION PAGE

Form Approved
OMB No. 0704-0188

1. REPORT DATE *(DD-MM-YYYY)*	**2. REPORT TYPE**	**3. DATES COVERED** *(From - To)*
August 2016	Technical Report/Final	

4. TITLE AND SUBTITLE

Evaluation of Electromagnetic Induction (EMI) Resistivity Technologies for Assessing Permafrost Geomorphologies

5a. CONTRACT NUMBER

5b. GRANT NUMBER

5c. PROGRAM ELEMENT NUMBER

6. AUTHOR(S)

Benjamin E. Barrowes and Thomas A. Douglas

5d. PROJECT NUMBER

5e. TASK NUMBER

5f. WORK UNIT NUMBER

7. PERFORMING ORGANIZATION NAME(S) AND ADDRESS(ES)

U.S. Army Engineer Research and Development Center (ERDC)
Cold Regions Research and Engineering Laboratory (CRREL)
72 Lyme Road
Hanover, NH 03755-1290

8. PERFORMING ORGANIZATION REPORT NUMBER

ERDC/CRREL TR-16-12

9. SPONSORING / MONITORING AGENCY NAME(S) AND ADDRESS(ES)

The ERDC Director's Office
3909 Halls Ferry Road
Vicksburg, MS 39180-6199

10. SPONSOR/MONITOR'S ACRONYM(S)

ERDC

11. SPONSOR/MONITOR'S REPORT NUMBER(S)

12. DISTRIBUTION / AVAILABILITY STATEMENT

Approved for public release; distribution is unlimited.

13. SUPPLEMENTARY NOTES

ERDC Center-Directed Research, "Integrated Technologies for Delineating Permafrost and Ground-State Conditions"

14. ABSTRACT

Effective and efficient mapping of permafrost subsurface composition at scales relevant to the design and maintenance of horizontal and vertical infrastructure has been a long-standing challenge. Of utmost utility would be the development of standoff measurement techniques that could discern at the meter to submeter spatial scale and up to 10 m into the subsurface the presence or absence of ice features. Ground-based geophysical measurement techniques, including ground penetrating radar, borehole logging, and electrical resistivity, have been used to interrogate the subsurface in permafrost terrains at the meters to kilometers scales. Airborne measurement techniques have broad applicability at the larger, kilometers to tens of kilometers scale and could support linear infrastructure development and terrain mapping. However, there is a broad need for cost-effective airborne geophysical techniques to obtain high-resolution measurements of specific areas of interest.

This report explores the potential application of airborne EMI methods for the investigation and mapping of permafrost and reviews current Engineer Research and Development Center (ERDC) EMI survey capabilities and new opportunities, including the development of a new medium-scale autonomous EMI instrument.

15. SUBJECT TERMS

Airborne, Electromagnetic induction, Frozen, Geomorphology, Geophysical surveys, Permafrost, Remote sensing, Resistivity, Scale, Scientific apparatus and instruments, Thaw

16. SECURITY CLASSIFICATION OF:			**17. LIMITATION OF ABSTRACT**	**18. NUMBER OF PAGES**	**19a. NAME OF RESPONSIBLE PERSON**
a. REPORT	**b. ABSTRACT**	**c. THIS PAGE**			**19b. TELEPHONE NUMBER** *(include area code)*
Unclassified	Unclassified	Unclassified	SAR	45	